SIMULATED RECORD VALIDATION VIA PREDICTION EQUATIONS FOR NONLINEAR SDOF RESPONSE

F. De Luca[1†], G. Ameri[2], I. Iervolino[1], F. Pacor[2], D. Bindi[3]

[1]*Dipartimento di Ingegneria Strutturale Università degli Studi di Napoli Federico II, Via Claudio, 21 80125, Naples, Italy.*

[2]*Istituto Nazionale di Geofisica e Vulcanologia, Via Bassini 15, 20133, Milan, Italy.*

[3]*Deutsches GeoForschungsZentrum GFZ, Centre for Disaster Managment (CEDIM), Telegrafenberg, 14473 Potsdam, Germany.*

ABSTRACT

Seismic structural risk analysis of critical facilities often asks for nonlinear dynamic analysis for which record selection is one of the key issues. Notwithstanding the increasing availability of databanks of strong-motion records, it may be hard to find records that fit a specific magnitude-distance scenario resulting from hazard assessment at the site of interest. Aimed at over passing the latter issue, a possible approach can be the use of artificial and/or simulated records in lieu of real records. The employment of such records requires systematical engineering validation in terms of structural response. Herein prediction equations for peak and cyclic inelastic single degree of freedom systems' response, based on Italian accelerometric data, are employed as a benchmark for the validation of synthetic records. This preliminary application is made on four simulated records for the 1980 M 6.9 Irpinia (Southern Italy) earthquake obtained with a broadband hybrid integral-composite technique. Results showed how this technique leads to acceptable results for the peak elastic and inelastic displacements, while less accurate response, with respect to the prediction equations, is found in terms of equivalent number of cycles. It is also shown that this kind of validation may provide different results with respect to classical signal-to-signal comparison of real and simulated records.

1. INTRODUCTION

Modern earthquake design and assessment procedures are based on assessment of inelastic deformations of structures. In this framework, nonlinear structural analysis methods have earned increasing interest in the scientific and professional communities. In particular, nonlinear dynamic analysis is becoming more common, especially for the design and the assessment of critical facilities (De Luca et al., 2011). Thus, ground motion selection methods improved significantly in accuracy (PEER, 2009). Notwithstanding the increased availability of strong-motion databanks, it may be difficult to find real records' sets that fit specific scenarios (e.g., large magnitude, small source-to-site distance). This lack records can be fulfilled by means of different approaches. One of the solutions can be to provide alternative seismic input, such as *artificial* or *simulated* accelerograms. However, the engineering use these kinds of records requires systematic validation (e.g., Bazzurro and Luco, 2004; Iervolino et al, 2010a). The target is to check whether the recorded motions can be substituted by those artificial or simulated, and in which situation such a replacement can be acceptable in terms of structural response.

The main target of engineering validation of "alternative" accelerograms should be to check whether these lead to the same probability of failure, or loss estimation, with respect to nominally equivalent real records, when employed in Performance Based Earthquake Engineering (PBEE), (i.e., Cornell and Krawinkler, 2000; Krawinkler and Miranda, 2004). The latter approach is an alternative perspective with respect to the direct, and more common,

† flavia.deluca@unina.it

comparison of real waveforms with their simulated counterpart. In fact, some signal mismatch may still be acceptable when considering the structural response. In this framework, intermediate validation steps (between visual record comparison and full risk assessment) are the real-to-simulated comparisons in terms of peak and cyclic nonlinear structural response of single degree of freedom (SDOF) systems (Iervolino et al, 2010a, Galasso et al., 2012), and the validation through prediction equations in terms of structural informative parameters such as the inelastic displacement (the objective of this study). It is to note that, all the real-to-simulated comparisons (even if made in terms of nonlinear structural response) are pursuable only when a real records' benchmark is available, while the validation through prediction equations does not need the real records correspondent to the simulation.

In the following, a first step towards the comprehensive validation of simulated records, outlined above, is provided. The set of synthetic accelerograms is calculated, for four sites that recorded the 1980 M 6.9 Irpinia earthquake (Ameri et al, 2011), with the broadband hybrid integral-composite (HIC) technique employing full-wavefield Green's function (Gallovic and Boreksova, 2007), recalled in the next section. The benchmarks are prediction equations in term of peak and cyclic inelastic intensity measures, IMs (De Luca 2011, De Luca et al., 2012), based on a constant strength reduction factor approach, are described in section three. The IMs selected are the peak inelastic displacement and the equivalent number of cycles. The relationships are developed for several nonlinear SDOF systems, based on the large set of ground motion data from the ITalian ACcelerometric Archive or ITACA (Luzi at al. 2008; Pacor et al., 2011). Results of validation, made on the basis of the prediction equations are provided in section four, along a direct (visual) real-to-simulated comparison, to emphasize the different conclusions that can be drawn.

2. GROUND-MOTION SIMULATION

The set of synthetic accelerograms adopted in this study is taken from Ameri et al. (2011). The authors, first modeled some ground motions recorded during the 1980 Irpinia earthquake in order to validate, from a seismological point of view, the generated synthetic seismograms. Then, several possible rupture processes of the Irpinia fault were considered, and the ground motion from these different "events", were calculated. This latter step was to capture the variability of the ground motion due to unknowns about the rupture. In particular, 54 different rupture processes were assumed for the this fault, considering 6 possible position of the hypocenter, 3 values of the velocity of the rupture propagation and 3 different distributions of the slip on the fault. These kinematic rupture parameters were assumed to vary according to the ranges reported in Ameri et al. (2011) and are selected in order to sample scenarios that could happen during the actual earthquake. For instance, some of the rupture processes may generate large motions at some sites due to directivity effects, or particularly high rupture velocity or proximity to a slip asperity. All the rupture scenarios are characterized by the same magnitude (Mw 6.9, the same as the 1980 earthquake) and the ground motion is simulated at different distances, according to the site locations. Thus, for each site a set of 54 synthetic accelerograms is available.

Four sites (Table 1), located at different distances and positions around the fault, have been selected. Moreover, since local site effects are not included in the simulations, those sites where chosen because, according to Ameri et al. (2011), local amplification doesn't significantly affect the ground motion. The adopted simulation methodology is here briefly described in order to stress that, differently from artificial or purely stochastic seismograms, the calculated synthetics are based on a more physical modeling of the earthquake source and wave propagation processes.

The HIC technique simulates the rupture process in terms of slipping of elementary subsources with fractal number-size distribution (fractal dimension 2), randomly placed on the fault plane (Zeng et al., 1994). At low frequencies, the source description is based on the representation theorem (integral approach, Aki and Richards, 2002), assuming a final slip distribution composed from the subsources, which is characterized by a *k-squared* decay (Herrero and Bernard, 1994; Gallovič and Brokešová, 2004). At high frequency, instead, the ground-motion synthesis is obtained summing the contributions from each individual subsource treated as a point source (composite approach). The Green's functions for both frequency bands are evaluated by the discrete wavenumber technique (Bouchon, 1981) in a layered 1D medium. This approach assures a broadband frequency content that satisfy the engineering needs. Moreover, as desirable, the model will produce coherent motion in the low-frequency band, generating for instance directivity pulses, and incoherent motion in the high-frequency one.

Table 1. Simulated records for the 1980 M 6.9 Irpinia earthquake (Ameri et al., 2011)

Station	Code	R_{epi} [km]	R_{JB} [km]	EC8 class
Bagnoli	BGI	22	7	B
Benevento	BNV	58	28	B
Bisaccia	BSC	28	18	A
Bovino	BVN	54	35	B

3. PREDICTIONS EQUATIONS OF NONLINEAR SDOF RESPONSE

It is a recent enhancement of Probabilistic Seismic Hazard Analysis or PSHA (McGuire, 2004) to express hazard in terms of nonlinear structural response measures; thus employing inelastic displacement of SDOF systems as an intensity measure in PBEE applications (e.g., Lawson, 1996; Borzi and Elnashai, 2000; Tothong and Cornell, 2006; Bozorgnia et al., 2010a and 2010b). PSHA carried out in terms of inelastic IMs provides the seismic threat at a site by means of a parameter more informative for engineering purposes. In fact, referring to the PBEE framework, previous studies (Tothong and Luco, 2007; PEER, 2009; Tothong and Cornell, 2007) showed that the inelastic displacement of SDoF systems is *efficient, sufficient* and *robust to scaling*, at least when seismic risk assessment of first mode dominated structures is of concern.

PSHA for nonlinear seismic response requires prediction equations for the parameters of interest; the semi-empirical models considered in this study (De Luca, 2011; De Luca et al., 2012), and considered in the following as a point of comparison for simulated records, were developed for SDOF systems whose backbones are characterized by bilinear with hardening behavior with and without stiffness' degrading in the hysteretic loops, named EPH-p and EPH-k respectively, see Figure 1(a).

Structural response measures include both cyclic (e.g., energy dissipation) and peak response (e.g., maximum inelastic deformation) quantities. Elastic periods of SDOFs range in a broad interval sampled by 20 values, from 0.04s to 2s. Level of nonlinearity is accounted for by considering different strength reduction factors (R_μ) equal to 2, 4, 6, 8. A constant strength reduction factor approach is adopted allowing every single record to show inelastic response; thus, the value of the yield strength (F_y) at a given oscillation period T is a record-specific quantity and it is computed according to Equation 1, being m the mass of the SDOF (always equal to 1 kg_{mass}) and $Sa_{el-record}(T)$ the ground motion elastic spectral acceleration at period T.

Two IMs were selected: the displacement-based parameter is the peak inelastic displacement (Sd_i), the cyclic response-related parameter is the equivalent number of cycles (N_e); Equation 2. The latter is given by the cumulative hysteretic energy (E_H), evaluated as the sum of the areas of the hysteretic cycles (not considering contribution of viscous damping), normalized with respect to the largest cycle, evaluated as the area underneath the monotonic backbone curve from the yielding displacement to the peak inelastic displacement ($A_{plastic}$); this allows separating peak demand, already considered in the first IM, from cyclic demand, (Manfredi, 2001).

$$F_y = \frac{F_{el}}{R_\mu} = \frac{Sa_{el-record}(T)\cdot m}{R_\mu} \tag{1}$$

$$N_e = E_H / A_{plastic} + 1 \tag{2}$$

The dataset is composed of 747 two-component waveforms from 103 earthquakes in the 4.1-6.9 moment magnitude (M_W) range, with hypocentral depth within 30 km, and recorded by 150 stations in the 0-200km distance range. The epicentral distance (R_{epi}), for M_W<5.5 events, and the closest distance to fault projection or Joyner and Boore distance (Joyner and Boore, 1981), R_{JB}, for stronger earthquakes, were considered, see Figure1(b). All stations are classified for site condition following Eurocode 8 or EC8 (CEN, 2004). Five soil type are considered: A, B, C, D, E. Most of site categories were assigned from geological and geophysical data (Di Capua et al., 2011) while about 30% from direct measurements of the value of the average shear wave velocity, $V_{S\,30}$.

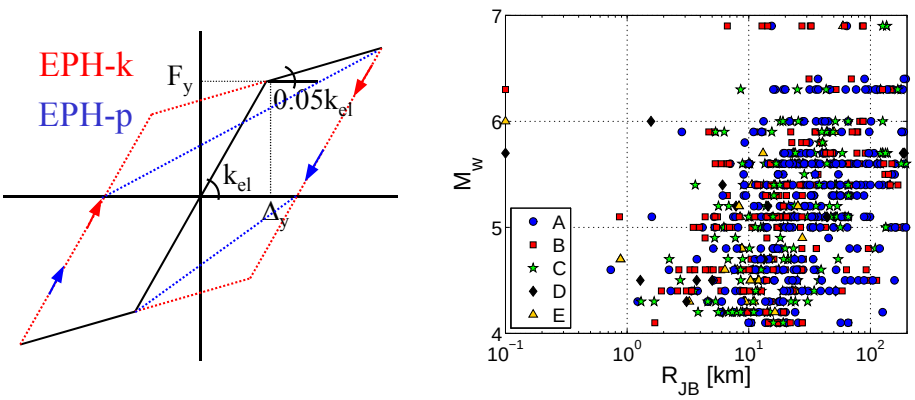

Figure 1. (a) EPH-k and EPH-p SDOF backbones; (b) magnitude versus distance (R_{epi} or R_{JB}) plot of the dataset, grouped according to the Eurocode 8 site classification.

The prediction equation models have the general form in Equation 3, being Y the geometric mean of the North-South and East-West components for Sd_i or N_e, a is a constant term, F_D, F_M, F_S, and F_{R_μ} are functions describing the distance, magnitude, site amplification, and nonlinearity dependence of the IMs. The specific expressions to be adopted in the case of Sd_i are F_{D1}, F_{M1}, while in the case of N_e are F_{D2}, F_{M2}, as shown in Equation 4 to Equation 7. Magnitude measure is M_W, distance is R_{JB}, or R_{epi} (in km). M_{ref}, M_h, R_{ref} are constants. The

term F_S is given by $F_S = s_j C_j$, for $j = 1,..,5$, where s_j are the coefficients, while C_j are dummy variables used to denote the five different EC8 site classes (A to E). The term F_{R_μ} is given by $F_{R_\mu} = r_k C_k$, for $k = 2,4,6,8$, where r_k are the coefficients, and C_k are dummy variables used to denote the four different strength reduction factors considered. In the regressions, the s_1 (corresponding to EC8-A site class) and r_2 (corresponding to R_μ=2) coefficients were constrained to be equal to 0.

As a side result, and employing the same functional form in Equation 3 to Equation 5, obviously excluding the F_{R_μ} term, also a prediction equation for elastic displacements ($Sd_{elastic}$) was obtained. Regression coefficients for elastic, inelastic displacements and equivalent number of cycles for EPH-k and EPH-p systems, not reported here for the sake of brevity, can be found in (De Luca 2011, De Luca et al., 2012).

An example of the performance of the predictive models is shown Figure 2, where the estimates for a magnitude 6.0 earthquake at two periods (T equal to 0.2s and 1.0s) are plotted as a function of distance for A site class and R_μ=4. The predictions are reported for both the considered systems (EPH-k and EPH-p) and they are compared with Sd_i or N_e data for a magnitude interval of 6.0±0.3. As expected the differences in the hysteretic loop between EPH-k and EPH-p systems have an effect only on cyclic response, while peak estimated are similar in the two cases.

$$\log_{10}(Y) = a + F_D + F_M + F_S + F_{R_\mu} \tag{3}$$

$$F_{D1} = \left[c_1 + c_2\left(M - M_{ref}\right)\right]\log_{10}\left(\sqrt{R_{JB}^2 + h^2}\,/R_{ref}\right) \tag{4}$$

$$F_{M1} = \begin{cases} b_1\left(M - M_h\right) + b_2\left(M - M_h\right)^2 & for\ M \le M_h \\ b_3\left(M - M_h\right) & otherwise \end{cases} \tag{5}$$

$$F_{D2} = c_1 \cdot \log_{10}\left(\sqrt{R_{JB}^2 + h^2}\,/R_{ref}\right) \tag{6}$$

$$F_{M2} = \begin{cases} b_1\left(M - M_h\right) & for\ M \le M_h \\ b_3\left(M - M_h\right) & otherwise \end{cases} \tag{7}$$

The standard deviation of residuals ($\sigma_{\log Y}$) associated to the median of the predictions equations are shown in Table 2 for elastic displacements ($Sd_{elastic}$), and inelastic displacements (Sd_i) and equivalent number of cycles (N_e) for both the EPH-k and EPH-p SDoF systems. For each IM considered the total (σ_{TOT}), the between-event (σ_B) and within-event (σ_W) standard deviations are shown as well. The evaluation of σ_B and σ_W is an enhancement presented in this study with respect to De Luca (2011) and De Luca et al. (2012) where only σ_{TOT} was given. The largest contribution to σ_{TOT}, for both the IMs and for both the SDOFs considered, is always given by within-event variability (σ_W), such contribution becomes more significant in the case of equivalent number of cycles.

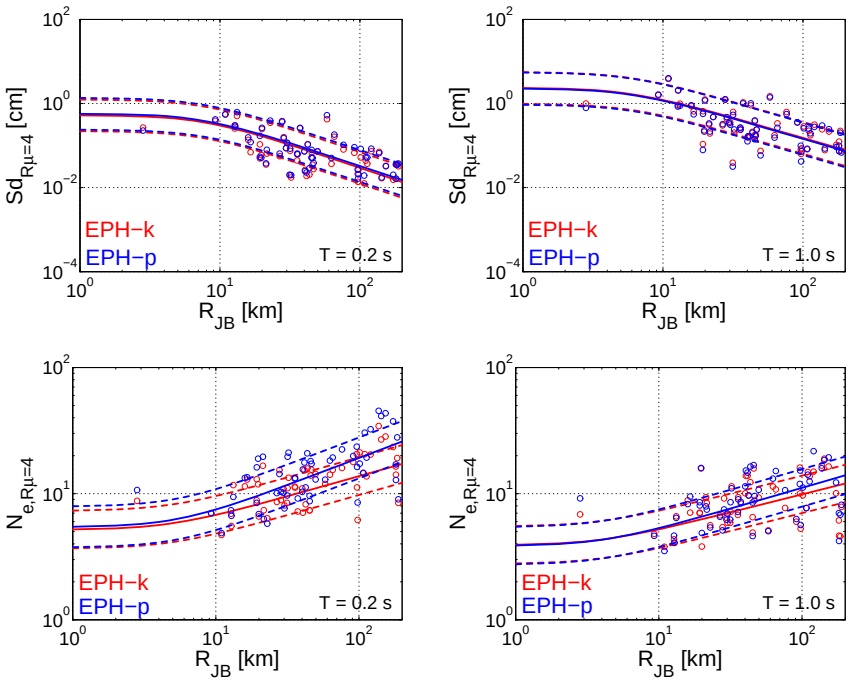

Figure 2. Sd_i and N_e estimates for a magnitude 6.0 earthquake, soil type A and R_μ equal to 4 at two natural periods (T = 0.2s and 1.0s) for both EPH-k and EPH-p systems, plotted as a function of R_{JB} and compared with the corresponding data for a magnitude interval of 6.0 ± 0.3.

Table 2. Standard deviation of residuals ($\sigma_{\log Y}$) associated to the median prediction on the models in Equation 2.

T[s]	$Sd_{elastic}$			$Sd_{i,EPH-k}$			$Sd_{i,EPH-p}$			$N_{e,EPH-k}$			$N_{e,EPH-p}$		
	σ_{TOT}	σ_B	σ_W	σ_{TOT}	σ_B	σ_W	σ_{TOT}	σ_B	σ_W	σ_{TOT}	σ_B	σ_W	σ_{TOT}	σ_B	σ_W
0.04	0.361	0.222	0.285	0.400	0.281	0.284	0.381	0.270	0.269	0.184	0.108	0.148	0.191	0.116	0.152
0.07	0.371	0.218	0.299	0.401	0.278	0.288	0.388	0.274	0.276	0.177	0.101	0.146	0.193	0.108	0.160
0.1	0.379	0.227	0.304	0.391	0.268	0.284	0.385	0.270	0.274	0.169	0.092	0.142	0.186	0.104	0.154
0.15	0.384	0.247	0.293	0.381	0.259	0.280	0.378	0.262	0.273	0.159	0.085	0.134	0.172	0.096	0.142
0.2	0.401	0.275	0.291	0.376	0.257	0.274	0.378	0.260	0.274	0.150	0.077	0.128	0.162	0.090	0.135
0.25	0.395	0.274	0.285	0.377	0.256	0.276	0.379	0.262	0.274	0.152	0.077	0.131	0.163	0.093	0.134
0.3	0.380	0.271	0.266	0.377	0.259	0.274	0.383	0.266	0.275	0.150	0.077	0.128	0.162	0.093	0.132
0.35	0.369	0.262	0.259	0.375	0.260	0.270	0.380	0.265	0.273	0.153	0.082	0.130	0.161	0.092	0.132
0.4	0.357	0.251	0.253	0.372	0.260	0.266	0.378	0.264	0.271	0.150	0.079	0.128	0.159	0.091	0.130
0.45	0.355	0.244	0.258	0.373	0.261	0.266	0.379	0.264	0.272	0.154	0.083	0.130	0.160	0.092	0.131
0.5	0.352	0.238	0.258	0.373	0.263	0.265	0.380	0.265	0.271	0.154	0.081	0.130	0.158	0.092	0.129
0.6	0.358	0.249	0.257	0.373	0.265	0.263	0.380	0.267	0.270	0.153	0.083	0.128	0.158	0.092	0.128
0.7	0.358	0.247	0.258	0.372	0.265	0.261	0.382	0.270	0.270	0.154	0.082	0.130	0.159	0.094	0.128
0.8	0.360	0.250	0.259	0.373	0.265	0.263	0.382	0.268	0.272	0.154	0.081	0.131	0.156	0.089	0.128
0.9	0.364	0.252	0.263	0.375	0.267	0.264	0.384	0.271	0.272	0.151	0.076	0.130	0.150	0.083	0.125
1	0.365	0.255	0.261	0.378	0.269	0.265	0.384	0.271	0.272	0.148	0.078	0.126	0.149	0.084	0.123
1.25	0.371	0.255	0.270	0.382	0.275	0.266	0.388	0.273	0.275	0.148	0.080	0.125	0.146	0.086	0.118
1.5	0.380	0.257	0.280	0.386	0.272	0.273	0.389	0.271	0.280	0.153	0.081	0.129	0.146	0.085	0.119
1.75	0.384	0.256	0.285	0.386	0.270	0.276	0.391	0.272	0.281	0.158	0.072	0.141	0.146	0.082	0.121
2	0.378	0.245	0.287	0.388	0.271	0.278	0.392	0.271	0.283	0.171	0.076	0.153	0.151	0.086	0.124

4. ANALYSES AND RESULTS

The preliminary validation provided herein is made on the accelerograms simulated at four sites for the 1980 M 6.9 Irpinia earthquake described in section 2 and employing as benchmark the prediction equations described in section 3.

Table 1 shows stations' identifiers, distances and EC8 soil classification of the sites. Figure 3 shows the first comparison in terms of $Sd_{elastic}$. In Figure 3 elastic displacement spectra are plotted for both the 54 simulated seismograms and the real records and compared with the estimates from the semi-empirical ground motion prediction equation (GMPE). The standard deviation bands are computed as $10^{m_{\log Y} \pm \sigma}$, in which $m_{\log Y}$ is the median estimate of the GMPE and σ is the standard deviation of the logarithm. Two different $\sigma_{\log Y}$ have been employed: the total standard deviation (σ_{TOT}) and within-event standard deviation (σ_W). The 54 simulations depict a significant variability of the elastic spectral ordinates that is produced by the variations of the kinematic rupture parameters. In the following, when referring to over or under estimation, it is meant that the simulated records are lower or higher than the median estimate, and they are outside the $\pm\sigma$ bands evaluated as described above.

For some periods and sites a systematic underestimation can be observed. However, this applies also to real records. In fact, the observed spectra (red curves) are always enclosed by simulated ones (grey curves). The results at BNV and BVN stations imply that the ground motion recorded from the Irpinia earthquake was smaller than that predicted by a GMPE developed for the whole Italian territory[‡].

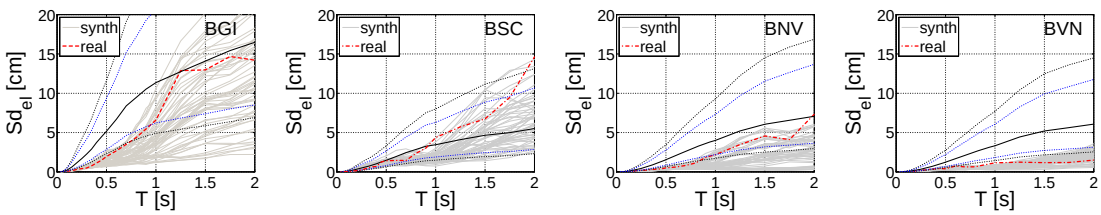

Figure 3. Median spectra of the prediction equation for $Sd_{elastic}$ with their $\pm\sigma_{TOT}$ (black dotted lines) and $\pm\sigma_W$ (blue dotted lines) bands compared with the corresponding spectra of the 54 simulated (*synth*) and the real (*real*) records at the stations BGI, BSC, BNV, and BVN.

Figure 4 shows the same plots provided in Figure 3, but in this case the comparisons are made in terms of Sd_i for EPH-k system, and $R_\mu = 4$ and $R_\mu = 8$. It can be observed that passing from elastic (Figure 3) to inelastic peak response (Figure 4) the trends are different. In the case of inelastic displacement at both $R_\mu = 4$ and $R_\mu = 8$, the 54 simulated records do not show the same level of underestimation. In the case of BNV and BVN stations an underestimation trend can still be recognized, yet it tends to attenuate with the increasing nonlinear behavior (form $R_\mu = 4$ to $R_\mu = 8$).

The preliminary comparison with the prediction equations in terms of peak elastic and inelastic response suggests that the simulated accelerograms generated with HIC technique can be an acceptable solution especially if the structural systems considered are characterized by

‡ It is also important to stress that only BGI record is included in the dataset employed for the estimation of the prediction equations.

high strength reduction factor. Such results find a strict analogy with the findings regarding peak inelastic response of stationary and non-stationary artificial records with respect to unscaled real records when code spectral matching is pursued (Iervolino et al, 2010a).

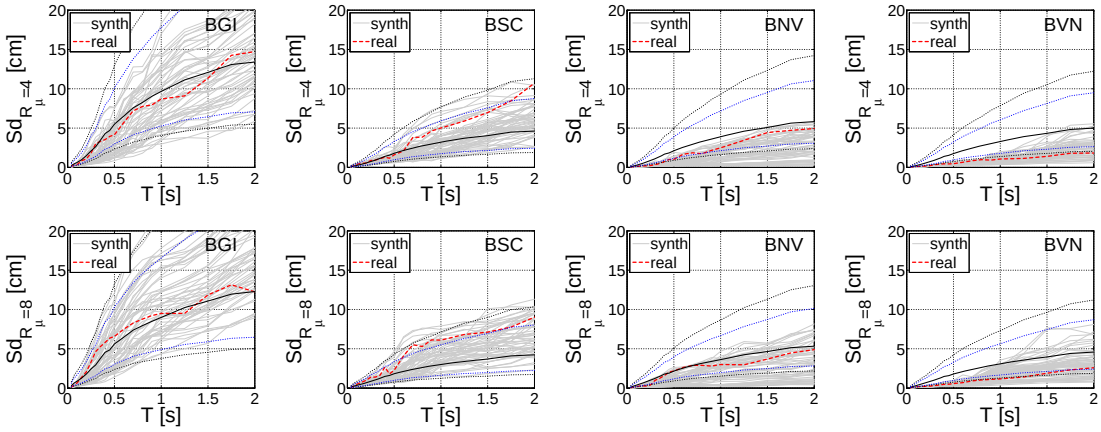

Figure 4. Median spectra of the prediction equation for Sd_i, EPH-k system, $R_\mu = 4$ and 8, with their $\pm\sigma_{TOT}$ (black dotted lines) and $\pm\sigma_W$ (blue dotted lines) bands compared with the corresponding spectra of the 54 simulated (*synth*) and the real (*real*) records at the stations BGI, BSC, BNV, and BVN.

In Figure 5 and Figure 6, N_e spectra are shown in the case of R_μ equal to 4 and 8, for both EPH-k and EPH-p SDOFs, respectively. In the case of cyclic response, the two SDOFs' backbone have been considered, given the differences observed in the median trends, and shown in the example in Figure 2. For both EPH-k and EPH-p, the 54 simulations provide a cyclic response systematically in the $-\sigma$ band of the GMPE (so systematically lower than the median estimate of the GMPE), and in some cases they are outside it. It is worth to be noted that also the real counterpart of the simulations (red dashed line in the figures) are mostly in the $-\sigma$ band of the GMPE.

The increasing strength reduction factor increases the underestimation observed in terms of cyclic response. Such an underestimation result is significantly different from the findings for spectral matched artificial records in which a statistically significant overestimation of the cyclic structural response was found (Iervolino et al, 2010a). This difference is quite expected because, in the adopted simulation, the waveforms are calculated solving the source and path durations according to the rupture and crustal propagation models considered. In particular, in the present case study, a one-dimensional crustal model is assumed which is likely also the cause of the average N_e underestimation. Indeed, the complexity of the Earth's crust produces a number of reflected and refracted waves that increase the overall duration of the seismogram with respect to a simple 1D model.

In Figure 7 a comparison of the relative errors of the median of the 54 simulations with respect to the median estimate of the GMPE (m_{synth} *vs GMPE*) and with respect to the real records (m_{synth} *vs real*) is shown for the case of elastic displacements and peak and cyclic inelastic response for R_μ equal to 4. The comparisons in Figure 7 emphasize the systematic underestimation in terms of both peak and cyclic response with respect to the GMPEs, already shown in Figures from 3 to 6.

The average value of the relative errors of the simulations with respect to the GMPE (m_{synth} *vs GMPE*) are around -50% for both peak and cyclic response. On the other hand such relative

errors assume a different significance in the two cases. In fact, while in terms of peak inelastic response the underestimation trend is between the $\pm\sigma$ bands of the GMPE (see Figure 4); similar values of the relative errors for the cyclic response lead to an underestimation, in most of cases, outside the $\pm\sigma$ bands of N_e prediction equations (see Figure 5 and 6).

The relative errors evaluated with respect to the real records emphasize a significant difference with the respect to the corresponding evaluations made in terms of GMPE in the case of inelastic displacements, while such differences tend to attenuate in the case of nonlinear response (both peak and cyclic).

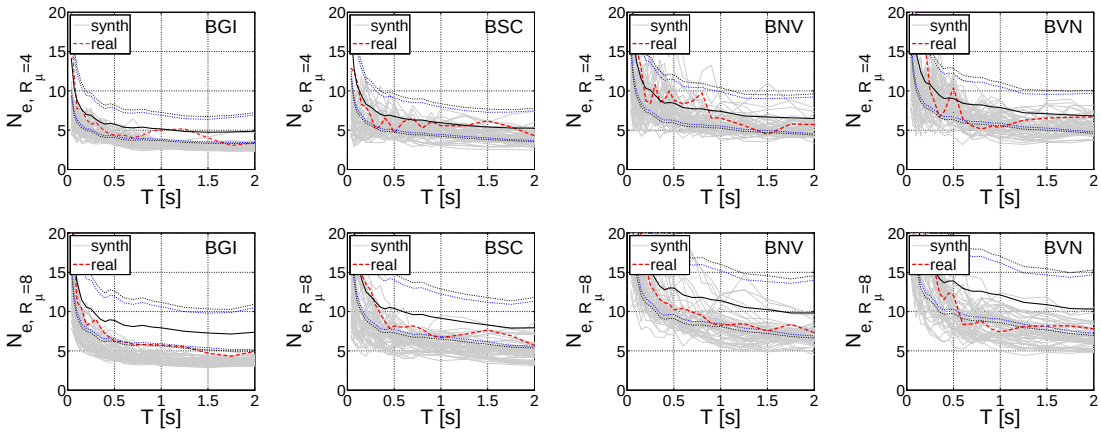

Figure 5. Median spectra of the prediction equation for N_e, EPH-k system, $R_\mu = 4$ and 8, with their $\pm\sigma_{TOT}$ (black dotted lines) and $\pm\sigma_W$ (blue dotted lines) bands compared with the corresponding spectra of the 54 simulated (*synth*) and the real (*real*) records at the stations BGI, BSC, BNV, and BVN.

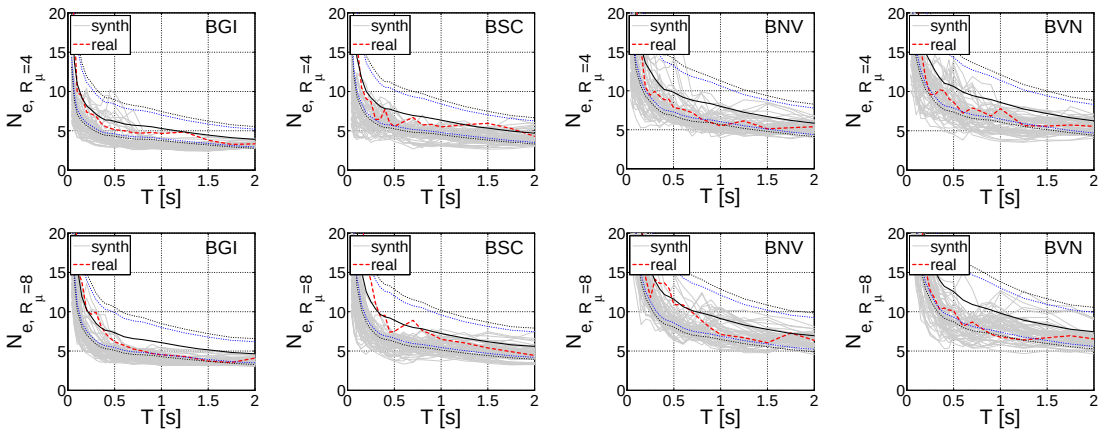

Figure 6. Median spectra of the prediction equation for N_e, EPH-p system, $R_\mu = 4$ and 8, with their $\pm\sigma_{TOT}$ (black dotted lines) and $\pm\sigma_W$ (blue dotted lines) bands compared with the corresponding spectra of the 54 simulated (*synth*) and the real (*real*) records at the stations BGI, BSC, BNV, and BVN.

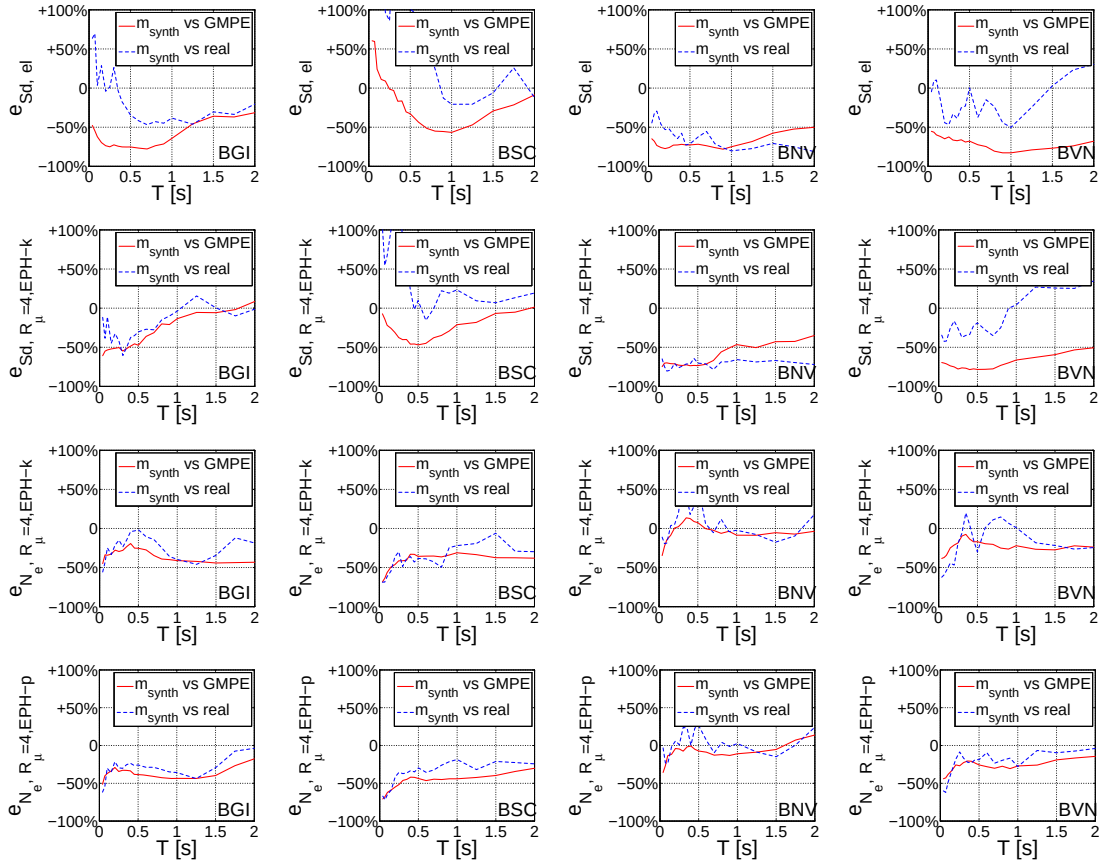

Figure 7. Relative errors of the median of the 54 synthetic records (m_{synth}) with respect to the median estimate of the prediction equation (*synth vs GMPE*) and with respect to real records (*synth vs real*) evaluated for $Sd_{elastic}$, Sd_i for the EPH-k system and N_e for both EPH-k and EPH-p systems for $R_\mu = 4$.

4. CONCLUSIONS

Prediction equations in term of peak and cyclic inelastic response can be employed as a benchmark for the engineering validation of simulated records. The validation made in terms of prediction equations has its main basis in the fact that as long as simulated records are employed in nonlinear dynamic analyses as substitutes of real records, the main target is that they lead to the same conclusion in terms of risk assessment.

A preliminary validation example, referred to the case of four sites for the 1980 Irpinia, M 6.9 earthquake was carried out focusing on the comparison of validation made by means of prediction equations with the more typical simulated-to-real validation approach.

In the example provided, elastic displacements, inelastic displacements, and equivalent number of cycles, for different strength reduction factors, were controlled as informative intensity measures for peak and cyclic response to be employed in the validation. The first, expected, conclusion is that considering nonlinear response rather than the only elastic one can provide additional significant results to the validation procedure.

The preliminary validation shows that the simulations have an underestimation trend mostly in terms of cyclic response with respect to the median estimates of the prediction equations. On the other hand, in the case of inelastic displacements the simulation are between the one

standard deviation band of the prediction equations.

The underestimation trend of the simulated records, observed in terms of peak and cyclic response, can be partially ascribed to the simplified simulation model with respect to the actual 3-dimensional crustal structure.

The underestimation of observed peak spectral displacement is similar, while the underestimation trend in terms of cyclic response is opposite, to what found in previous studies for spectrum-compatible artificial records.

Notwithstanding the preliminary character of the results provided, given the small sample of records considered; the validation approach through prediction equations of peak and cyclic inelastic response is a first step towards a systematical engineering validation of physics-based simulated accelerograms.

ACKNWOLEDGEMENTS

The study presented in this paper have been developed within the activities of the *Rete dei Laboratori Universitari di Ingegneria Sismica – ReLUIS* for the research program funded by the *Dipartimento della Protezione Civile* (2010-2013).

REFERENCES

Abrahamson N.A., Youngs R.R., 1992. A stable algorithm for regression analyses using the random effects model. Bulletin Seismological Society of America, 82, 505–510.

Aki, K., and P. G. Richards (2002). Quantitative Seismology, Second Ed. University Science Books, Sausalito, California, 704 pp.

Ameri G., Emolo A., Pacor F., Gallovic F., 2011. Ground-motion simulations for the 1980 M 6.9 Irpinia earthquake (southern Italy) and scenario events. Bulletin Seismological Society of America, 101, 1136–1151.

Atkinson G.M.,Goda K, 2010. Inelastic Seismic Demand of Real versus Simulated Ground-Motion Records for Cascadia Subduction Earthquakes Bulletin Seismological Society of America, 100(1), 102-115.

Bazzurro P., Luco N., 2004. Post-elastic response of structures to synthetic ground motions. Report for Pacific Earthquake Engineering Research (PEER) Center Lifelines Program Project 1G00 Addenda. CA, US.

Bindi D., Pacor F., Luzi L., Puglia R., Massa M., Ameri G., Paolucci R., 2011. Ground motion prediction equations derived from the Italian strong motion database, Bulletin of Earthquake Engineering, 9(6), 1899-1920.

Borzi B., and Elnashai A.S., 2000. Refined force reduction factors for seismic design, Engineering Structures, 22, 1244–1260.

Bouchon, M. (1981). A simple method to calculate Green's functions for elastic layered media, Bull. Seismol. Soc. Am. 71, 959–971.

Bozorgnia Y., Hachem M.M., Campbell K.W., 2010a. Ground motion prediction equation ("attenuation relationship") for inelastic response spectra. Earthquake Spectra 26(1), 1-23.

Bozorgnia Y., Hachem M.M., Campbell K.W., 2010b. Deterministic and probabilistic predictions of yield strength and inelastic displacement spectra. Earthquake Spectra 26(1), 25-40.

Comité Européen de Normalisation (CEN), 2004. Eurocode 8 – Design of Structures for earthquake resistance – Part 1: General rules, seismic actions and rules for buildings. EN 1998-1, CEN, Brussels.

Cornell, C.A. and Krawinkler, H. , 2000. Progress and challenges in seismic performance assessment. PEER News, April 2000.

De Luca F., 2011. Records, capacity curve fits and reinforced concrete damage states within a performance based earthquake engineering framework. PhD thesis. Department of Structural Engineering, University of Naples Federico II. Advisors: G. Manfredi, I. Iervolino, G.M. Verderame. Available at http://wpage.unina.it/iuniervo/

De Luca F., Ameri G., Iervolino I., Pacor F., Bindi D., 2011. Prediction equations of nonlinear SDOF response: towards an enhanchment of hazard analysis. 30° Convegno Nazionale GNGTS - Gruppo Nazionale di Geofisica della Terra Solida, 14-17 Novembre, 2011.

De Luca F., Ameri G., Iervolino I., Pacor F., Bindi D., 2012. Prediction equations for peak and cyclic engineering seismic response based on Italian data. Earthquake Spectra, (under review).

Di Capua G., Lanzo G., Pessina V., Peppoloni S., Scasserra G., 2011. The recording stations of the italian strong motion network: geological information and site classification. Bulletin of Earthquake Engineering, 9(6), 1779-1796.

Galasso C., Zareian F., Iervolino I., Graves R.W., 2012. Validation of ground motion simulations for historical events using SDOF systems, Bulletin of the Seismological Society of America (under review).

Gallovič, F., and J. Brokešová (2004). The k^{-2} rupture model parametric study: Example of the 1999 Athens earthquake, Studia geoph. et geod. 48, 589–613.

Gallovič, F., and Brokešová J., 2007. Hybrid k-squared source model for strong ground motion simulations: Introduction, Physics of the Earth and Planetary Interiors, 160, 34–50.

Hancock J., Bommer J.J., Stafford P.J., 2008. Number of scaled and matched accelerograms required for inelastic dynamic analyses. Earthquake Engineering and Structural Dynamics, 37(14), 1585-1607.

Herrero, A., and P. Bernard (1994). A kinematic self-similar rupture process for earthquakes, Bull. Seismol. Soc. Am. 84, 1216–1228.

Iervolino I., De Luca F., Cosenza E., 2010a. Spectral shape-based assessment of SDOF nonlinear response to real, adjusted and artificial accelerograms, Engineering Structures, 32, 2776-2792.

Iervolino I., Giorgio M., Galasso C., Manfredi G., 2010b. Conditional hazard maps for secondary intensity measures, Bulletin of Seismological Society of America, 100(6), 3312-3319.

Joyner W.B., Boore D.M., 1981. Peak horizontal acceleration and velocity from strong-motion records including records from the1979 Imperial Valley, California, earthquake, Bulletin of Seismological Society of America 71, 2011–2038.

Krawinkler H. and Miranda E., 2004. Performance-Based Earthquake Engneering. In: Bozorgnia Y. and Bertero V.V. Editors Earthquake Engineering: From engineering seismology to performance-based engineering, CRC Press, chapter 9.

Lawson, R. S., 1996. Site-dependent inelastic seismic demands, Ph.D. Thesis, Department of Civil Engineering, Stanford University, Stanford, CA.

Luzi L., Hailemikael S., Bindi D., Pacor F., Mele F., Sabetta F., 2008. ITACA (ITalian ACelerometric Archieve): A web portal for the dissemination of Italian strong-motion data, Seismological Research Letters, 79, 716-722.

Manfredi G., 2001. Evaluation of seismic energy demand, Earthquake Engineering and Structural Dynamics, 30(4), 485–499.

McGuire R.K., 2004. Seismic hazard and risk analysis. Report MNO-10. Earthquake Engineering Research Institute Publication, Oakland, CA, USA.

Pacor F, Paolucci R, Ameri G, Massa M, Puglia R, 2011. Italian strong motion records in ITACA: overview and record processing. Bulletin of Earthquake Engineering, 9(6), 1741.1759.

PEER ground motion selection and modification working group – Haselton C.B., editor, 2009. Evaluation of Ground Motion selection methods: prediction median interstory drift response of buildings. PEER report 2009/01.

Tothong P., Cornell C.A:, 2006. An empirical ground-motion attenuation relation for inelastic spectral displacement. Bulletin of the Seismological Society of America, 96(6), 2146-2164.

Tothong P., Cornell C.A:, 2007. Probabilistic seismic demand analysis using advanced ground motion intensity measures, attenuation relationships, and near fault effects. John A. Blume Earthquake Engineering Center, Department of Civil and Environmental Engineering, Stanford University, CA 2007.

Tothong P., Luco N., 2007. Probabilistic seismic demand analysis using advanced ground motion intensity measures. Earthquake Engineering and Structural Dynamics, 36, 1837-1860.

Zeng, Y., J. G. Anderson, and G. Yu (1994). A composite source model for computing realistic synthetic strong ground motions, Geophys. Res. Lett. 21, 725–728.